28. Sharp, K. A. and Honig, B., *Curr. Opin. Struct. Biol.*, 1995, **5**, 323–328.
29. Troll, M., Roitman, D., Conrad, J. and Zimm, B., *Macromolecules*, 1986, **19**, 1186–1194.
30. Falk, M., Hartman, K. A. Jr. and Lord, R. C., *J. Am. Chem. Soc.*, 1962, **84**, 3843–3846.
31. Chapman, R. E. and Sturtevant, J. M., *Biopolymers*, 1969, **7**, 527–537.
32. Lo Surdo, A., Alzola, M. and Millero, F. J., *J. Chem. Thermodyn.*, 1982, **14**, 649–662.
33. Hershey, J. P., Damesceno, R. and Millero, F. J., *J. Solution Chem.*, 1984, **13**, 825–841.
34. Spiro, T. G., Revesz, A. and Lee, J., *J. Am. Chem. Soc.*, 1968, **90**, 4000–4006.
35. Williams, R. K. and Epand, R. M., *J. Phys. Chem.*, 1986, **90**, 1413–1416.
36. Wu, J. Q. and Macgregor, R. B. Jr., *Biochemistry*, 1993, **32**, 12531–12537.
37. Marmur, J. and Doty, P., *J. Mol. Biol.*, 1962, **5**, 109–118.
38. Thomas, R., *Biochim. Biophys Acta*, 1954, **14**, 231–238.
39. Dove, W. F. and Davidson, N., *J. Mol. Biol.*, 1962, **5**, 467–478.
40. Kotin, L., *J. Mol. Biol.*, 1963, **7**, 309–311.
41. Krakauer, H., *Biochemistry*, 1974, **13**, 2579–2589.
42. Lyons, J. W. and Kotin, L., *J. Am. Chem. Soc.*, 1964, **86**, 3634–3640.
43. Hamaguchi, K. and Gelduschek, E. P., *J. Am. Chem. Soc.*, 1962, **84**, 1329–1338.
44. Friedman, H. L., *Annu. Rev. Phys. Chem.*, 1981, **32**, 179–204.
45. Hilbert, R., Doctoral Dissertation, University of Karlsruhe, Karlsruhe, West Germany.

ACKNOWLEDGEMENTS. The unorthodox thinking, as Prof. P. Ganguly, Head of the Division advocated in many informal chats has inspired me to think on a variety of 'apparently un-connected issues'. I gratefully acknowledge Prof. Ganguly's precious gift. I also thank an anonymous reviewer for frutiful suggestions rendering this article more intelligible.

Received 13 March 1996; revised accepted 16 July 1996.

**RESEARCH ARTICLE**

# Electrical resistivity imaging of Mohand Anticline of Siwalik range: A tectonic appraisal

**Ch. Sivaji, B. R. Arora*, R. Kalra and A. K. Pandey**

Indian Institute of Geomagnetism, Colaba, Bombay 400 005, India
*Present address: Department of Space Geophysics, National Institute of Space Research, Sao Jose dos Campus, Brazil.

**The results of a pilot resistivity sounding experiment undertaken in the Siwalik belt and contiguous Indo-Gangetic Foredeep (IGF) are presented and their lithotectonic significance is discussed akin to the Mohand anticlinal structure. The inferred large lateral resistivity contrast near Ganeshpur delineates the concealed Mohand thrust. The observed resistivity doublet is compatible with the transition in the clast–size and clast–matrix ratio of conglomerate to sandstone. This correspondence provides strong geophysical support to the proposed four stage evolutionary model of the Mohand Siwalik basin on the basis of the facies association and palaeocurrent data. Cyclic pattern of resistivity distribution seen in the Mohand–Sherpur sector of IGF is considered to manifest episodic character of tectonic events in the Himalayan orogeny.**

THE Indian Institute of Geomagnetism has been carrying out the natural source electromagnetic investigations in the Himalayas and the adjoining shield region[1–3]. These studies, employing magnetovariational and magnetotelluric techniques, image the deep crustal structures in terms of electrical conductivity (inverse of resistivity) distribution. The strong dependence of conductivity on temperature prevailing at deeper depths and the fluid content released and remobilized by the metamorphic and tectonic processes, makes these investigations a sensitive pointer of the geodynamic process controlling seismic and tectonic activity in the collision regime. These visualizations are well illustrated by the noted correlation of the mapped Trans-Himalayan and Garh-

wal Lesser Himalaya conductivity anomalies with the high seismicity zones[4,5]. With the objective of supplementing information from shallow depths, it was decided to introduce control source deep electrical resistivity surveys. At shallow depths, the resistivity distribution being more sensitive to the state of saturation and/or to the fractured rock fabrics of the medium, the knowledge of resistivity distribution can effectively be used to infer the control of proximal or distal tectonics on the nature of sedimentation in the foredeep basins as well as in the alluvial fan system developed at the base of rising mountain system. We report in this paper the experimental details and results of a pilot resistivity survey undertaken in and around the Mohand structure of Siwalik range, Garhwal Sub-Himalaya.

## Tectonic features of the study area and electrical sounding locations

For the resistivity sounding experiment, a section of the Siwalik range bounded between Yamuna and Ganga tear faults was selected. This section of the Siwalik fold belt lying on the southern flank of the Dehradun valley has received much attention from the Earth scientists for its anticlinal structure, Mohand anticline. The gentle NE dipping strata of the Siwalik range here show a sharp reversal of dip on its southern limit, giving the appearance of an anticline with its axis roughly aligned in NW–SE direction. The lithological sequence in the Siwalik range is represented by sandstone/mudstone couplets at the base, followed by multistoried sandstone complex and capped up by boulder conglomerate, respectively classified as Lower, Middle and Upper Siwalik[6]. Due to the anticlinal uplift, the Upper Siwalik in the crest region is extensively eroded, exposing the underlying Middle Siwalik on the SE flank. The Upper Siwalik are exposed on the NE flank abutting against the alluvium deposits of Dehradun valley. On the SE margin, the Siwalik range terminates into the Indo-Gangetic Foredeep (IGF). The contact boundary between the Siwalik range and alluvial deposits of the IGF, regionally called as Main Frontal Thrust or more simply as Himalayan Foothill Boundary (HFB)[7], is locally referred to as Mohand Thrust. This thrust is inferred to be concealed under the alluvium deposit[8,9]. The presence of the Mohand Thrust at depth was confirmed by borehole lithology encountered in structural and deep wells drilled by the Oil and Natural Gas Commission (ONGC) to evaluate hydrocarbon prospects of the Siwalik range[8].

Four Schlumberger electrical soundings were conducted respectively at Kotri, Dharmawala, Ganeshpur and Sherpur (Figure 1) so as to provide maximum possible coverage of Mohand anticline. The first two sounding lines were located respectively on the southern and northern limb of the anticline. The Kotri sounding line is located some 14 km northwest of Mohand whereas the Dharmawala sounding is on the northeastern flank of the anticline, close to the contact boundary of Upper Siwalik conglomerate sequence with alluvium. Both these sounding lines run parallel to the general NW–SE strike of the Mohand anticline. The Ganeshpur sounding line is located very close to the boundary between the alluvium and Siwalik with sounding line striking across the Mohand thrust. The fourth resistivity sounding line, centered near village Sherpur, was situated deep within the IGF, some 15 km south of Ganeshpur on the Dehradun–Saharanpur road.

The large variations in the range of apparent resistivities observed between Sherpur and Ganeshpur soundings warranted us to conduct axial dipole sounding to locate the lateral inhomogeneity between these locations.

## Data acquisition and reduction

The Schlumberger resistivity sounding technique, adopted here, employs a co-linear electrode configuration symmetrically disposed to the central sounding point. A DC current I, in the form of square wave interrupted for the required time intervals through commutator switches, is injected into the ground by means of outer pair of electrodes $A$ and $B$. The other pair of non-polarizable electrodes, $M$ and $N$, placed close to the central point, is used to measure the potential difference, $\Delta V$, resulting from the current flow. An apparent resistivity, $\rho_a$[10–12], is given by

$$\rho_a = \frac{\Pi[(AB)^2 - (MN)^2]}{4MN} \cdot \frac{\Delta V}{I}$$

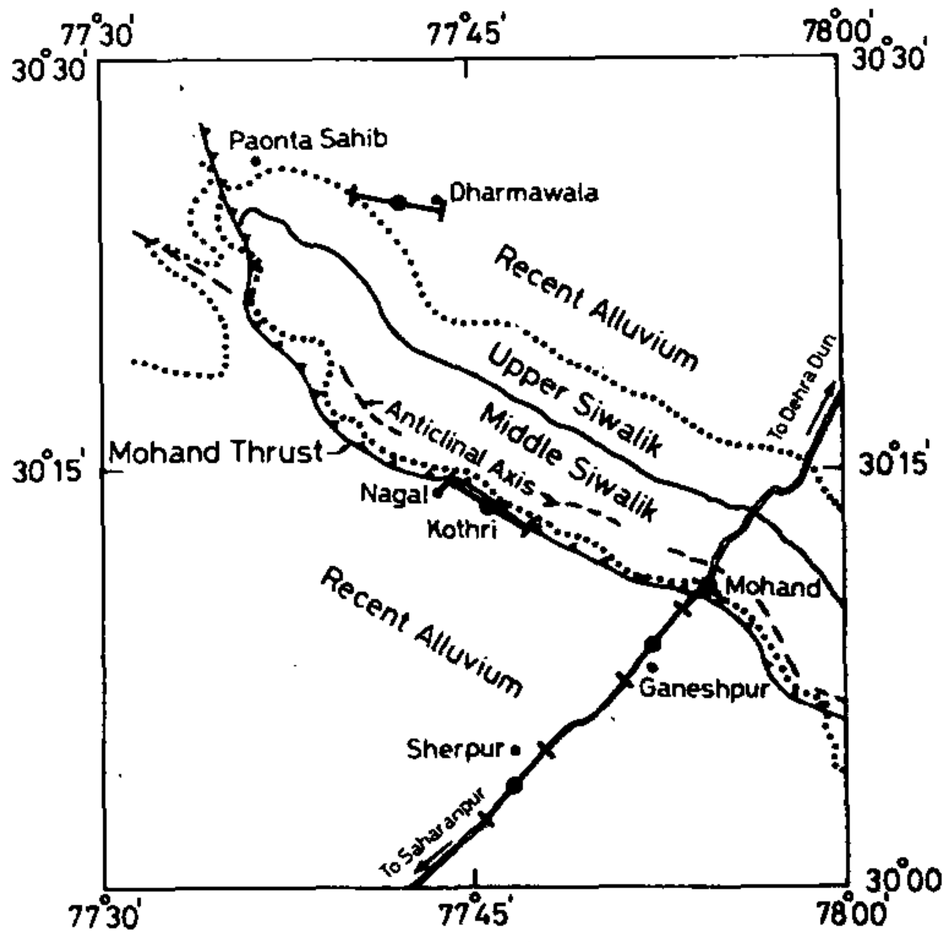


**Figure 1.** Map of study area showing the location of deep resistivity sounding lines on the Dehradun–Saharanpur road, undertaken to image electric resistivity distribution around the Mohand anticlinal structure.

The current electrode separation is increased systematically to achieve progressively deeper penetration. While moving apart the current electrodes in successive observations, the potential electrodes are kept fixed for a large number of the *AB* settings. The change in *MN* spacing is introduced only when the potential drop across the *MN* falls with increasing *AB* separation to a value close to the limiting precision of the receiver unit. This restricted repositioning of the potential electrodes helps to minimize the distortions resulting from the localized near-surface resistivity inhomogeneities. These effects, termed electrode effects[13], could pose serious problem in the present case as the study region exposes a wide range of geological formations. The ratio of potential and current electrode separation was maintained between 1:5 and 1:10. This choice ensured adequate voltage drop across *MN* for the entire range of *AB*s.

The field measurements were accomplished with the Scintrex Resistivity Sounding equipment, essentially consisting of a current transmitting unit TSQ-4 backed up by 10 kW motor generator and a voltage measuring unit IPR-8. The motor generator generates three phase 210 Volts (AC) with a frequency of 600 Hz. This energy is transformed according to a front panel voltage setting in a large transformer housed in TSQ-4. The resulting AC is then rectified in a rectifier bridge. The commutator switch controls the DC voltage output in the square waveform interrupted at required time intervals. The IPR-8 receiver has a built-in facility to cancel self-potential existing at the potential electrodes. Driving the source current from generator and transmitter, maximum *AB* separation of 6 km was attained.

The apparent resistivity obtained as a function of electrode separation *AB*/2 is plotted on the log–log scale to give usual representation of sounding curve. With a suitable choice of geometrical progression of current electrodes, a fairly uniform distribution of points on the sounding curve was obtained. The raw electrical sounding data as recorded at the Sherpur is shown in Figure 2. Often various segments of the sounding curve, each corresponding to a particular *MN* spacing, exhibit slight vertical shift in relation to adjacent branches. This invariably manifests the electrode effect associated with the repositioning of the *MN* electrodes, also due to the lateral inhomogeneities encountered between previous and present *MN* spacing. Since measurements with larger *MN* spacing involve larger volumes, they provide better average information. The shift in adjacent sections of the sounding curve is corrected by vertically shifting the segment of the sounding curve with smaller *MN* spacing so as to provide fit to the section of the sounding curve with larger *MN* spacing[11,14]. Figure 2 demonstrates such a shift correction applied to the Sherpur sounding data. With these shift corrections, the overall shape of the sounding curve remains unaltered and only such smooth

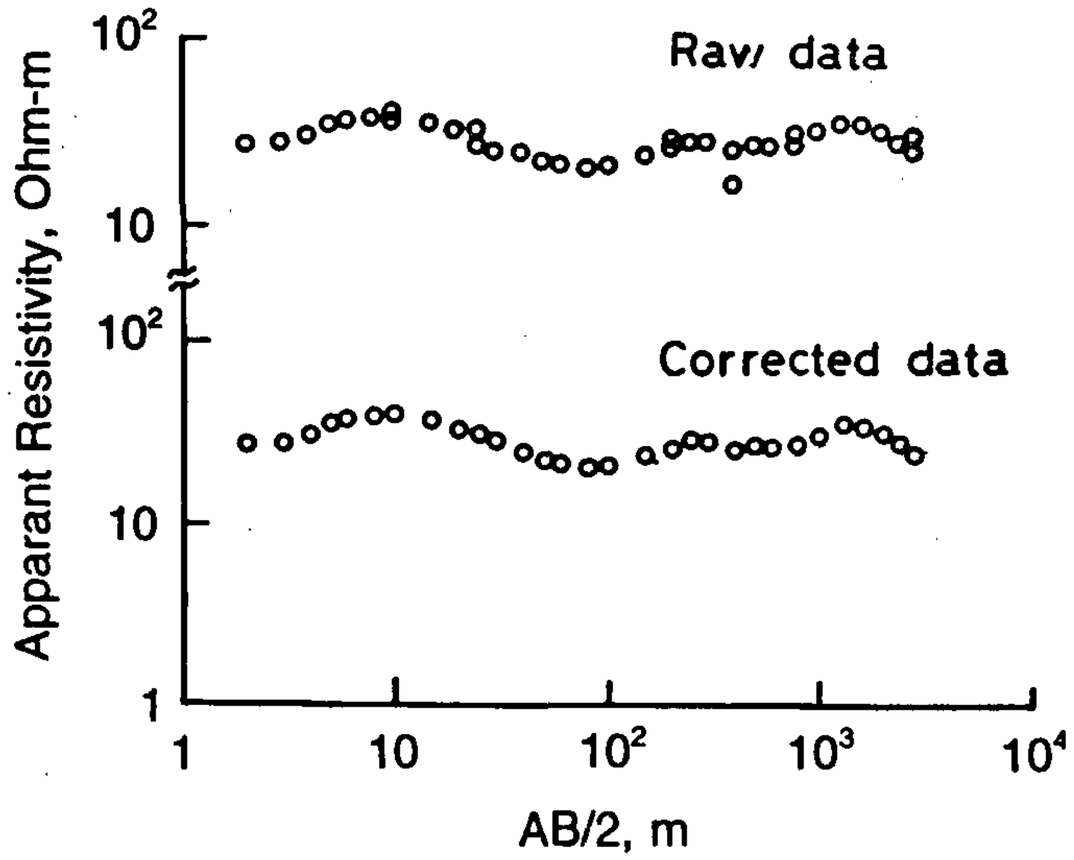


**Figure 2.** Plot of apparent resistivity vs electrode separation (*AB*/2) at Sherpur: as reduced from raw data (top) and after correcting (bottom) for electrode effect seen as vertically shifted segments of sounding curve.

sounding curves are used for subsequent interpretation of a 1-D layered structure.

For the two axial dipole soundings conducted, the current electrodes with 2 and 2.8 km separation were kept fixed while the potential electrodes with constant separation of 700 m were successively moved along the axis of current dipole with radial distances varying from 2 to 8 km on either side of the centre of the current dipole. The values of apparent resistivity for each position of potential dipole, calculated using the formula given below, were plotted as a function of radial distance of potential dipole from the central position of current electrodes to depict lateral variation of apparent resistivity along the line of movement.

The apparent resistivity is computed for the axial dipole configuration by the formula

$$\rho_a = \frac{\Pi R^3}{AB.MN} \cdot \frac{\Delta V}{I},$$

where $R$ is the radial distance from the centre of the current dipole to the centre of potential dipole.

The axial sounding up to a radial distance of 8 km on either side of the Sherpur and Ganeshpur was undertaken with potential electrodes deployed approximately at every 2 km. Figure 3 shows the lateral variation obtained from two axial dipole soundings, the implications of which are discussed in the foregoing sections.

## Numerical interpretation of sounding curves

The corrected apparent resistivity sounding curves have been interpreted by two different approaches, viz. the

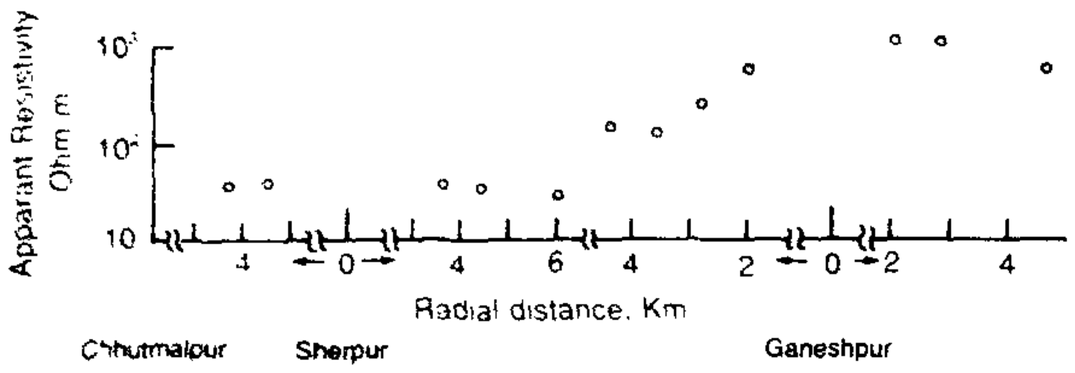


**Figure 3.** Plot showing the lateral variation in resistivity as obtained by axial-dipole soundings at Sherpur and Ganeshpur.

Marquardt–Levenburg[15] and Occam's inversion[16]. The Marquardt–Levenburg (M–L) formulation interprets the resistivity data in terms of horizontal layer of isotropic resistivity. The method incorporating *a priori* information on the number of layers as well as initial approximations on layers parameters (thickness and resistivity), performs an iterative process to refine the model parameters while minimizing the sum of the squares of residuals between observed and calculated responses. The Occam's inversion, on the other hand, yields a smooth resistivity–depth model minimizing the integrated square of the first or second derivative of resistivity values with respect to the depth. This approach reduces the ambiguity in fixing up the number of layers in the layered-structured model of the Earth.

Figure 4 *a–d* shows the interpreted layered as well as smooth continuous resistivity–depth distribution models for all the four soundings conducted around the Mohand structure. The degree to which these models explain the data is illustrated in Figure 5 *a–d* by superposing the calculated response of the best fitting models, both layered as well as continuous, on the observed sounding data, separately for all profiles. The comparative study of these models revealed that the maximum and minimum in the Occam's model corresponded well with the resistivities of the layers seen as zones of relatively high and low resistivities. Further, the sharp resistivity discontinuities represented by layer boundaries match well with the inflection points between minima and maxima observed in the Occam's model. The correlation between the reduced resistivity models, obtained by the two techniques, provided confidence in the model parameters. Their primary features are summarized below:

### *Kotri and Dharmawala soundings*

The Kotri and Dharmawala soundings, respectively on the southern and northern limb of the Mohand anticline, present a nearly consistent picture. The Kotri sounding with a thin overburden of modest resistivity (70 ohm.m) indicates a high resistivity layer of about 550 ohm.m

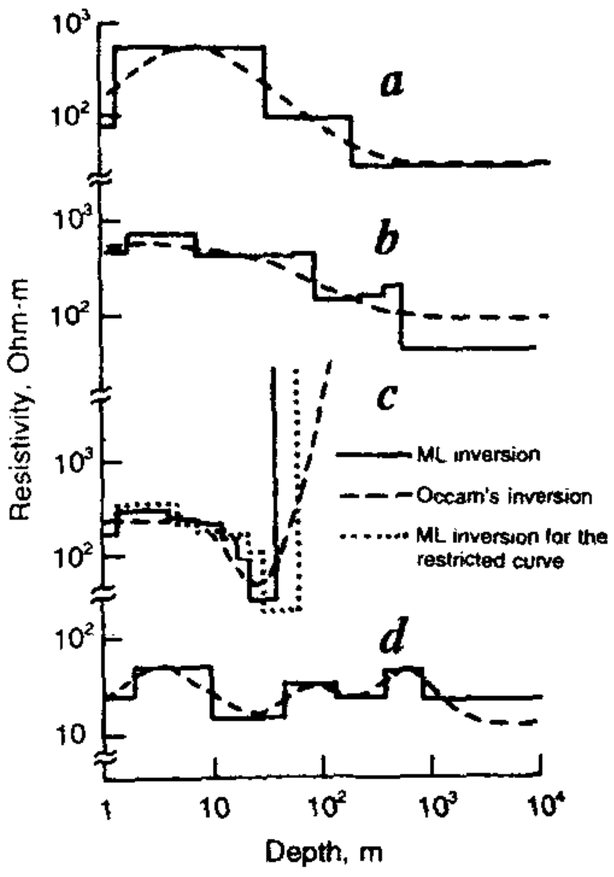


Fig. 4

**Figure 4 *a–d*.** Interpreted layered (solid line) as well as continuous resistivity-depth distribution (broken-line) models for resistivity sounding curves at (*a*) Kotri, (*b*) Dharmawala, (*c*) Ganeshpur and (*d*) Sherpur. For Ganeshpur, results are based on the interpretation of restricted (dotted line) and full (broken) sounding curve (see text).

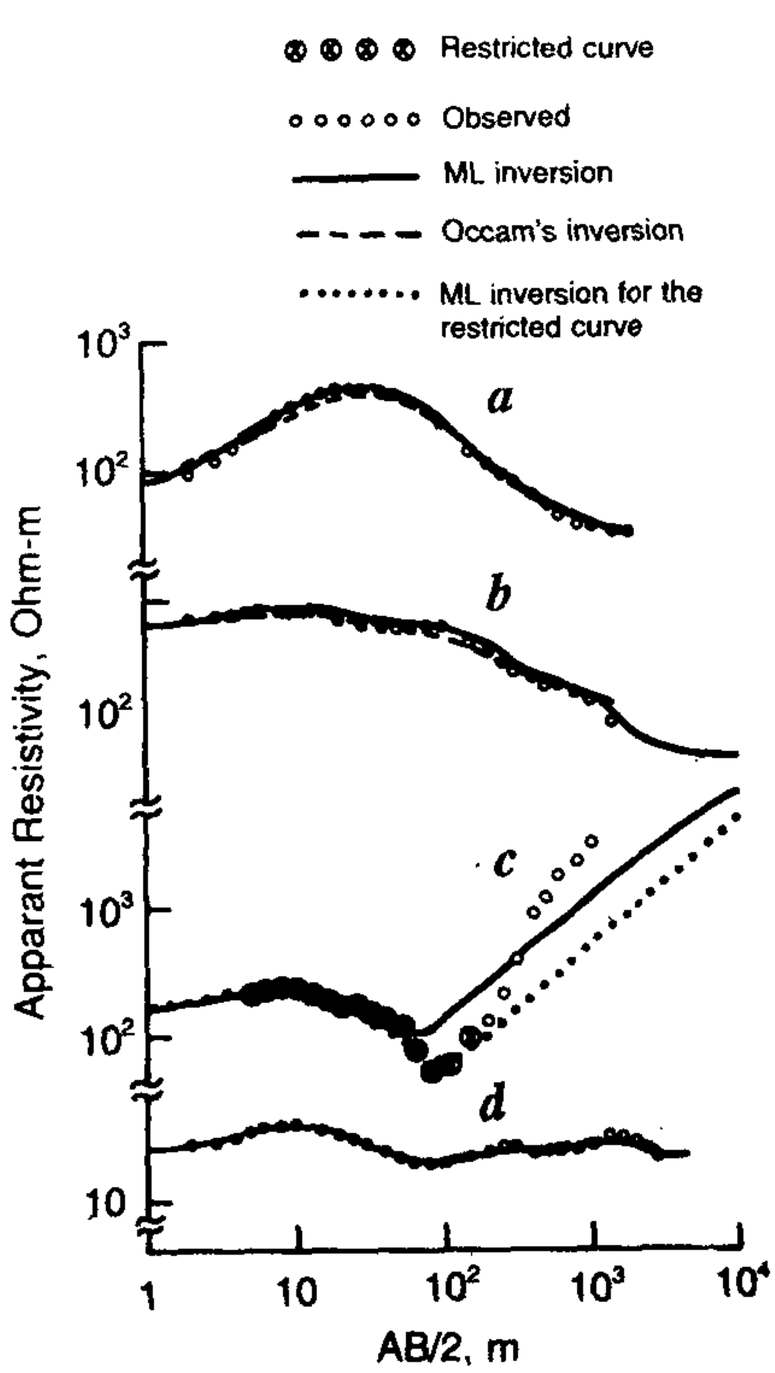


**Figure 5 *a–d*.** Plots showing calculated responses of best fitting layered (solid) and continuous depth-resistivity (broken line) models, shown in Figure 4, to the observed data (hollow circles) at (*a*) Kotri, (*b*) Dharmawala, (*c*) Ganeshpur and (*d*) Sherpur. For Ganeshpur and Sherpur, the Occam's and *ML*, inversion fits are overlapping and hence the broken line cannot be shown separately. The dotted line represents *ML*, fit for the restricted part of the curve indicated by crossed circles.

having an approximate thickness of 30 m (Figure 4 *a*). The interpretation of the Dharmawala sounding indicates near-equivalent resistivity (ranging between 425 and 740 ohm.m) layer at the surface, extending up to the depth of about 90 m (Figure 4 *b*). On both the soundings, this high resistivity layer is underlain by a relatively less resistive layer. The 4th layer on the Kotri profile has resistivity of nearly 90 ohm.m. This layer is not resolved by the Dharmawala sounding. Of the four soundings operated, the Dharmawala sounding is most strongly affected by the electrode effects. This, coupled with high contact resistance at the current electrodes, has greatly reduced the depth penetration of current. The non-detection of the moderately resistive layer at Dharmawala may be the effect of this restricted penetration, although the presence of such a layer cannot be ruled out by the continuously decreasing trend of the sounding curve at large electrode separation.

### *Sherpur sounding*

In marked contrast to the soundings located on the Mohand anticline, the Sherpur sounding profile located only 15 km south of the HFB into the Indo-Gangetic foredeep, is characterized by low resistivities. Here the resistivity–depth distribution, in the upper 1000 m section, is represented by an 8-layered structure (Figure 4 *d*). The resistivity of the individual layers ranges between a narrow range of 17 and 50 ohm.m, a distinct feature being that resistivity distribution alternates between relatively low and high resistivity layers. The layer of lowest resistivity (17 ohm.m) extending from 10 m depth, with a thickness of approximately 40 m, appears to represent the aquifer. The depth of this layer is in good agreement with the depth of the water table as revealed by the existing wells in the vicinity of the sounding.

### *Ganeshpur sounding*

The Ganeshpur sounding, placed close to the HFB, exhibits an H-type curve (Figure 5 *c*), symbolizing the presence of a low resistive layer sandwiched between resistive layers. However, the sounding curve when the electrode separation *AB* exceeds 100 m, rises very steeply. Both the Occam and *M–L* inversion schemes fail to yield a single model providing match for the complete sounding curve (Figure 5 *c*), especially the steeply rising segment. The last segment of the sounding curve will be asymptotic to a line rising at an angle 45° when the lowermost layer is an insulator[10,12]. However, the observed slope of the experimental sounding curve at Ganeshpur is more than 45° which cannot be explained even by the insulated bottom layer. Hence, this may be visualized as a diagnostic of the presence of large lateral electrical resistivity contrast at shallow depth along the sounding line. The interpretation of the Ganeshpur sounding curve up to an electrode separation of 100 m by the *M–L* algorithm, indicated that this section of the sounding curve is compatible with a top resistive layer of 200–300 ohm.m underlain by a low-resistivity layer of 20 ohm.m with an approximate thickness of 33 m extending from the 30 m depth. Assigning these values to a 3-layer model, with only the resistivity of the infinite third layer as a free parameter, the *M–L* algorithm was made to search by iterative process the resistivity which could provide the closest fit to the rising part of the Sherpur sounding curve. It was found that even when the bottom layer attains a value of the order of 20,000–25,000 ohm.m, the overall fit is not satisfactory and also the match to the first section of the sounding curve is seriously distorted (see Figure 5 *c*). This exercise demonstrated that even a near-insulating substratum at a shallow depth of 60–70 m is not consistent with observations, providing further credence to the hypothesis of large lateral resistivity inhomogeneity. It can be surmised that as the current with increasing current electrode separations tends to penetrate to the depth of the discontinuity, the capacitor-like behaviour of the electrical inhomogeneity tends to drain away the electrical energy (R. J. Sporry, personal communication), resulting in the steep rise of sounding curve after certain threshold of the electrode separation.

It is noteworthy that estimated depth of low resistivity zone (20 ohm.m), obtained by modelling the curtailed sounding curve, agrees well with the water level in a single well located only a few meters away from the sounding centre. Comparison with Sherpur model suggests that aquifer located at 10 m depth deepens to a depth of 30 m near Ganeshpur.

## Axial dipole sounding

The results of the axial soundings provide independent confirmation of the lateral resistivity inhomogeneity, a little north of Ganeshpur. The examination of lateral variation plot of resistivity in Figure 3, as estimated from the axial dipole sounding centered at the Ganeshpur, indicates that apparent resistivity on the northeast part is more than 1000 ohm.m as compared to the apparent resistivity of 200–300 ohm.m on the SW part. The axial dipole sounding results centered at the Sherpur revealed uniform value between 30 and 40 ohm.m on either side. These results indicate that near-homogeneous resistivity distribution in the IGF tends to be progressively inhomogeneous as the HFB is reached, with HFB marking zone of sharp resistivity contrast. The deduced lateral resistivity distribution shows good semblance with the exposed lithology of the area. The alluvium-covered region of the IGF is marked by low

and laterally uniform resistivity whereas the transitional and high-resistivity zones respectively match the pebble mixed alluvium and boulder sequence of the region.

## Geological and tectonic bearings

The results of the present resistivity sounding experiment indicate that Mohand Thrust, marked by large lateral resistivity contrast, is located in close proximity to the centre of Ganeshpur sounding. The thrust is indicated to be concealed approximately at a depth of about 40–50 m. Due to the known sensitivity of control source electrical method to resolve resistive structure[4], the electrical resistivity soundings elsewhere on the Mohand anticline have been able to divide upper pile of sedimentary sequence into a multiple layer sequence. Figure 6 summarizes the results of resistivity soundings in the form a geological cross-section corresponding to shallow depths. The picture of deeper section is adapted from Raiverman *et al.*[7].

In agreement with the exposed lithology, the top resistive layer (~550 ohm.m) at Dharmawala is shown to correspond with the boulder-bearing sequence of the Upper Siwalik. Extending the analogy, the second resistive layer at Kotri with similar resistivity character is also identified in Figure 6 as boulder dominated conglomerate sequence. Both at Dharmawala and Kotri, this layer is underlain by a relatively lower resistivity (200 ohm.m) layer. Making in-depth examination of the stratigraphic sections in and around Mohand Siwalik, Kumar and Ghosh[6] identified four distinct facies association occurring vertically upward as A (sandstone-mudstone), B (sandstone), C (sandstone-conglomerate) and D (conglomerate) the facies association C and D occurring mostly in the Upper Siwalik.

They observed that facies association C is characterized by stratified conglomerate with clast-ratio determined by 30–50% of conglomerate and 40–60% of sandstone. The facies association C gradually passes upward into poorly-imbricated conglomerate sequence in which conglomerate : sandstone ratio changes to 70:30. The clast size also varies from 10–25 cm in facies association C to 25–40 cm in association D. It is interesting to note that resistivity changes observed between resistive doublet at Dharmawala and Kotri are compatible with this transition in the clast–size and the clast–matrix ratio, the upper resistive and underlying relatively less resistive layers respectively representing formations dominated by facies D and C.

Clearly, the ability of the control source electrical method to sub-divide the Upper Siwalik sequence into two distinct layers, arising due to lithological change, can be considered as geophysical support to the four-stage evolution model of Mohand Siwalik basin, proposed by Kumar and Ghosh[6], with two stages of sedimentation occurring during Upper Siwalik.

At Kotri, this resistive doublet is sandwiched between moderately resistive layers of 70–150 ohm.m. These resistivities are typical of sandstone[17] and are interpreted as representing the sandstone sequence of Middle Siwalik. While the lower layer may mark the Middle Siwalik sequence brought close to surface by compressional forces responsible for anticlinal structure, the top moderately-resistive layer is considered to denote the debris derived from the erosion of Middle Siwalik exposed near the crest of anticlinal structure. Further south, near Ganeshpur, the contact between the concealed resistive Upper Siwalik and alluvium deposit may provide the kind of lateral resistivity contrast mapped by Ganeshpur sounding and axial dipole resistivity surveys. Compressional stresses associated with anticlinal folding may also cause weak flexing of the basement in the immediate vicinity of the southern limb of the anticline and may account for the deepening of the water-bearing sedimentary column as compared to the Sherpur. The subsequent filling of this basin-like structure with the boulders brought down by rising Mohand anticline may provide surface cover, seen here as a surfacial resistive (200 ohm.m) layer near Ganeshpur, concealing the contact between Siwalik and alluvium. Intermixing with the channelized or braided river deposits may lower the resistivity of this boulder sequence as compared to the Upper Siwalik boulder conglomerates seen on the limbs of the anticline.

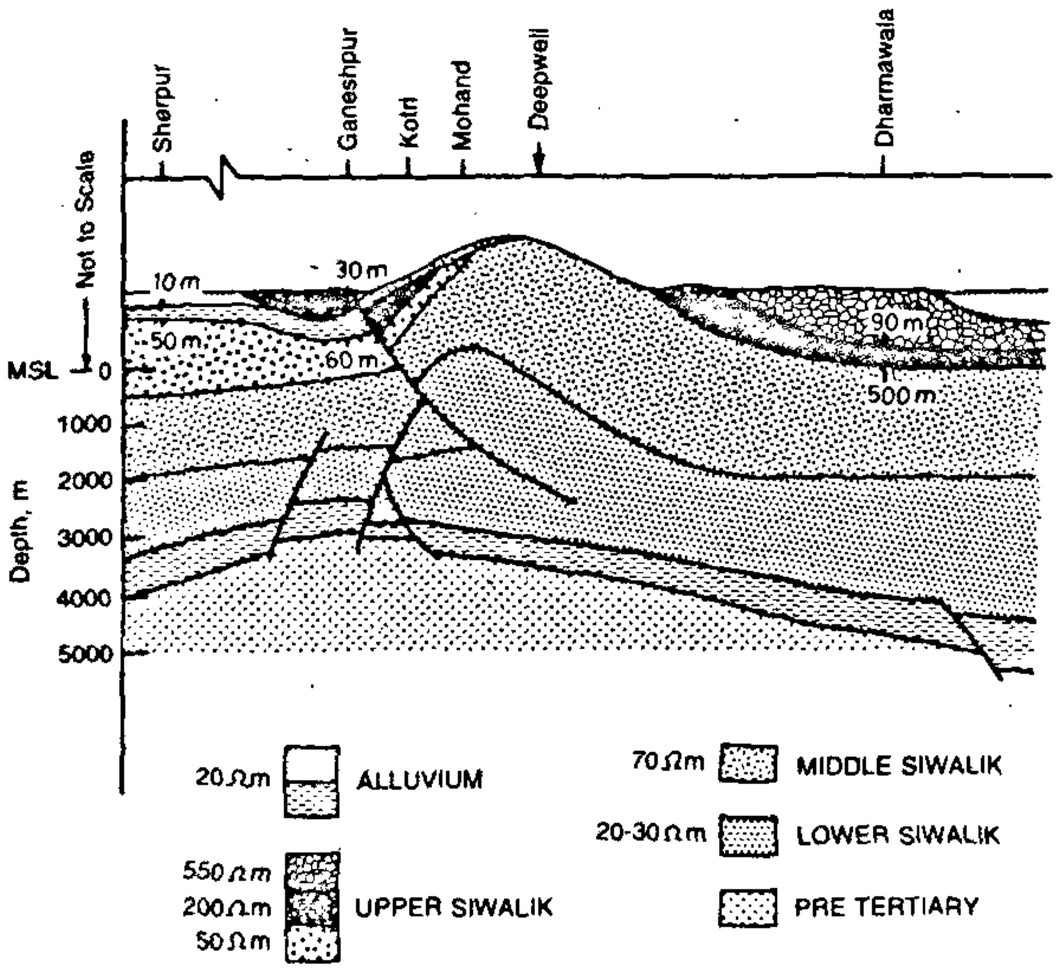


**Figure 6.** Schematic geological cross-section across the Mohand anticlinal structure, incorporating features of electrical resistivity distribution estimated from the present study. The vertical scale for shallow section is highly exaggerated but depths of mapped interfaces at each of the sounding sites are shown. The deeper section is adapted from Raiverman *et al.*[7].

The most interesting feature of the resistivity–depth distribution at Sherpur is the repetition of high and low resistivity couplet. Since the development and nature of sedimentation in the foredeep basin is largely caused and constrained by the tectonic history of the orogen, it is tempting to relate their cyclic distribution of resistivity to the episodic tectonism in the evolution of the Himalaya. The high resistivity layer may be visualized as coarse-grained sedimentary formation due to the rapid tectonic impulses. Superimposed on this is the slow sedimentation during a long quiescent period. The slow sedimentation results in fine-grained rock formations symbolizing the low resistive layers. Further, Bhattacharya and Misra[18] conclude that during most of the middle Siwalik times, the sands were being deposited by streams due to the floods at repeated intervals. They have also visualized that the Upper Siwaliks were deposited under the proglacial conditions in the Mohand area by streams originating from melt waters at the ice front of mountain glaciers. Sinha[9] pointed out that the sediments of the Siwalik of Mohand were derived from some mobile belt occurring towards east and northeast and consisted of igneous and metamorphic rocks of the Himalayan belt. This mobility, a series of episodic tectonic events, is a manifestation of the general uplift of the Himalaya during the post-Oligocene periods[19].

The relatively low resistivities of all the layers in the IGF as compared to the Siwaliks may be due to the moist conditions prevailing in the foredeep. However, the alternative resistivity highs and lows can be effectively correlated to the episodic tectonic events in the Himalayan belt, if a comprehensive study on the integrated geological and geophysical data is attempted in this sector of Indo-Gangetic Foredeep.

## Conclusions

A pilot electrical resistivity survey in and around the Mohand structure has unambiguously located the Mohand thrust. Elsewhere the mapped resistivity distribution is compatible with the lithology and has been helpful in constraining the geological cross-section of the Mohand structure at shallow depths.

The top Upper Siwalik sequence on the NE flank is seen as a resistive doublet. Similar doublet embedded between relatively less resistive layers is identified on the SW flank.

This might warrant that during the anticlinal upliftment, Upper Siwalik sequence may not have been completely eroded on the SW flank. The exposed sandstone sequence on this flank may simply be the debris of eroded Middle Siwalik from the crest region beneath which lies the normal Upper and Middle Siwalik sequence.

The cyclic distribution of resistivity at Sherpur may be visualized as manifestation of the episodic tectonism.


1. Arora, B. R. and Singh, B. P., *Mem. Geol. Soc. India*, 1992, **23**, 223–263.
2. Arora, B. R., Mahashabde, M. V. and Reddy, C. D., Project Completion Report, submitted to DST, 1995, pp. 120.
3. Gupta, G., Gokarn, S. G. and Singh, B. P., *Phys. Earth Planet. Inter.*, 1994, **83**, 217–224.
4. Arora, B. R. and Mahashabde, M. V., *Phys. Earth Planet. Inter.*, 1987, **45**, 119–127.
5. Reddy, C. D. and Arora, B. R., *J. Geomagn. Geoelectr.*, 1993, **45**, 775–785.
6. Kumar, K. and Ghosh,. S. K., *Himalayan Geol.*, 1994, **15**, 143–159.
7. Raiverman, V., Srivastava, A. K. and Prasad, D. N., *Himalayan Geol.*, 1993, **4**, 237–256.
8. Rao, Y. S. N., Rahman, A. A. and Rao, D. P., *Himalayan Geol.*, 1974, **4**, 137–150.
9. Sinha, R. N., *J. Geol. Soc. India*, 1970, **11**, 163–170.
10. Keller, G. V. and Frischknescht, F. C., *Electrical Methods in Geophysical Prospecting*, Pergamon Press, New York, 1966, pp. 90–196.
11. Kunetz, G., *Principles of Direct Current Resistivity Prospecting*, Gebruder Bortraeger, Berlin, 1966, 1–103.
12. Telford, W. M., Geldart, E. P. and Sheriff, R. E., *Applied Geophysics*, Cambridge University Press, Cambridge, 1990, pp. 522–577.
13. Constable, S. C., McElhinny, M. W. and McFadden, P. J., *Geophys. J. R. Astron. Soc.*, 1984, **79**, 893–910.
14. Zijl, J. V. S. van, *A Practical Manual on the Resistivity Method*, Geophysics Division, NPRL, CSIR, Pretoria, 1985, pp. 1–136.
15. Vander Valpin, B. P. A. and Sporry, R. J., *Comput. Geosci.*, 1993, **19**, 691–703.
16. Constable, S. C., *Geophysics*, 1987, **52**, 289–300.
17. Rao, M. B. R., *Outlines of Geophysical Prospecting–A Manual for Geologists*, Prasaranga, Manasagangotri, Mysore, 1975, p. 9.
18. Bhattacharya and Misra, *Beitr. Mineral. Petrograph.*, 1963, **9**, 211–214.
19. Krishan, M. S., *Geology of India and Burma*, Higginbothams, Madras, 1960, pp. 542–558.


ACKNOWLEDGEMENTS. We thank the staff of the Geological Survey of India, Northern Region, Lucknow, for their help in field practice and in upkeeping of Resistivity unit. We also thank the Director of the home Institution and the Division of the Earth System Sciences, Department of Science and Technology, New Delhi for the facilities provided.

Received 15 April 1996; revised accepted 5 July 1996